

3 criteria (Reisberg *et al.*, 1982). After following the subjects for 1–3 years, amnesic MCI subjects showing AD-like metabolic changes (decreased CMRglc in the temporoparietal areas and posterior cingulate) were found to be at risk for conversion to AD.

Follow-up FDG-PET has not been performed in CDR 0.5 subjects, but follow-up with other approaches has indicated that CDR 0.5 subjects with a higher CDR-sum of boxes (SB) score more frequently decline to AD compared with those with lower CDR-SB scores (Morris *et al.*, 2001). CDR 0.5 subjects with a higher SB score also show decreased metabolism in AD-specific areas (Perneczky *et al.*, 2007). These results suggest that CDR 0.5 converters to AD have an AD-like metabolic pattern, and the aim of this study was to examine this hypothesis using FDG-PET in our MCI/CDR 0.5 cohort.

The Osaki-Tajiri Project, previously called the Tajiri Project, is a community-based program on stroke, dementia, and bed-confinement prevention in Osaki, northern Japan. In our Prevalence Study 1998 (Meguro *et al.*, 2002), we reported rates of CDR 0.5 and MCI of 30.1% and 4.9%, respectively, with CDR 0.5 having a significantly greater prevalence (Meguro *et al.*, 2004). Among the participants in Prevalence Study 1998, we were able to examine CMRglc for 68 people and follow them for five years, after which we examined the incidence of dementia that developed in CDR 0 and 0.5 subjects (Incidence Study 2003; Meguro *et al.*, 2007). In the current study, we investigated whether the baseline CMRglc of CDR 0.5 converters to dementia manifests as metabolic changes specific to early AD.

Methods

Participants

In Prevalence Study 1998, 564 adults from among an epidemiologic population of 1,654 were randomly selected to undergo MRI (1.5T, Shimazu, Japan). The cost of all the MRIs was officially borne by the town. Finally, 497 participants agreed to undergo MRI: 346 CDR 0 (healthy), 119 CDR 0.5 (questionable dementia), and 32 CDR 1+ (dementia) subjects. T1-weighted (TR/TE 400/14) and T2-weighted (TR/TE 3000/90) images were used for assessing atrophy and cerebrovascular diseases, as described previously (Meguro *et al.*, 2002).

Owing to the limited time available for FDG-PET examination at Tohoku University Cyclotron Radioisotope Center (an average of four patients a month), we had to select subjects who would

receive PET. From the 497 subjects who underwent MRI, we randomly selected 35 CDR 0 (10% of 346) and 60 CDR 0.5 (50% of 119) subjects, and all 14 AD patients among the CDR 1+ group, for PET. Finally, we were able to examine 68 subjects using PET: 14 CDR 0, 42 CDR 0.5, and 12 AD. The other subjects refused to undergo PET examinations due to "psychological" reasons and the travelling distance between the community and the PET center (a one-hour drive).

All AD patients had a rating of CDR 1 and met the NINCDS-ADRDA criteria for probable AD (McKhann *et al.*, 1984). All CDR 0.5 subjects showed mild cognitive dysfunction, but this did not affect their daily lives in the community and none met the DSM-IV criteria for dementia (American Psychiatric Association, 1994). All 68 subjects met the following inclusion criteria: (1) no history of stroke, head injury or systemic disorders that could affect brain function, and normal values of vitamin B₁, B₆, B₁₂, folate, and thyroid hormones; (2) no cerebrovascular diseases as shown by MRI, and no marked neurological signs and symptoms; and (3) agreement of the subjects and family members to participate in Incidence Study 2003 and to be followed for five years.

Written informed consent was obtained from all CDR 0 and 0.5 subjects and from the families of CDR 0.5 and AD patients. The study was approved by the Ethical Committee of the Cyclotron Radioisotope Center of Tohoku University and the Tajiri SKIP Center.

CDR assessment

A clinical team of doctors and public health nurses determined the CDR while blinded to the cognitive tests (see below) and PET findings. Before being interviewed by the doctors, public health nurses visited the participants' homes to evaluate their daily activities. Observations by family members regarding the participants' lives were described in a semi-structured questionnaire; for participants who lived alone, public health nurses visited them frequently to evaluate their daily lives. The participants were interviewed by doctors to assess episodic memory, orientation, problem solving and judgment. Finally, the CDR stages were decided at a joint meeting, with reference to the information provided by the family. A reliable Japanese version of the CDR Work Sheet (Meguro, 2004) has been established, and one of the authors (K.M.) has been certified as a CDR rater at the Alzheimer's Disease Research Center, Washington University School of Medicine. CDR 0.5 participants who converted to AD were classified as CDR 0.5/converters and those who did not convert as CDR 0.5/non-converters.

The CDR was evaluated using the same approach at baseline and follow-up.

Cognitive assessment

A team of trained psychologists performed cognitive tests while blinded to the CDR stages and PET findings. These tests included the Mini-mental State Examination (MMSE; Folstein *et al.*, 1975) and the Cognitive Abilities Screening Instrument (CASI) (Teng *et al.*, 1994). The CASI has nine domains: long-term memory, short-term memory, attention, concentration/mental manipulation, orientation, visual construction, abstraction and judgment, list-generating fluency, and language. The long-term memory domain evaluates knowledge and remote memory, and herein we refer to this domain as "remote memory." The short-term memory domain assesses delayed recall of three words presented orally and immediate recall of five objects presented visually, and we refer to this domain as "recent memory."

PET

The PET study was performed with a model PT931/04-12 scanner (CTI Inc., USA; axial/transaxial resolutions: 8 mm) using [¹⁸F]fluorodeoxyglucose (FDG) (Phelps *et al.*, 1979; Reivich *et al.*, 1979). A short cannula was placed in a radial artery for blood sampling. Each subject was positioned with the OM line parallel to the detector rings according to brain slices collected by MRI. A cross of light was projected onto marks on the subject's head, which were set at standard points of 30 mm and 77 mm above and parallel to the OM line. A 20-minute transmission scan was performed using a ⁶⁸Ge/⁶⁸Ga external ring source. Thirty to 45 minutes after injection of 5–12 mCi of FDG, two emission scans were performed and data were collected simultaneously from each of seven contiguous axial sections. A total of 14 slices parallel to the OM line with a thickness of 6 mm were analyzed, encompassing virtually the whole brain. The detailed methodology has been described previously (Yamaguchi *et al.*, 1997).

Imaging analyses

ROI

After two different pairs of axial T1-weighted MRI and PET images were matched with each other at the same brain slice, the position of the regions of interest (circular ROIs, 2.7 cm²) were defined manually using the overlapped images. A total of 13 ROIs in each hemisphere were selected: upper frontal, anterior frontal, inferior frontal, parietal, temporo-parieto-occipital, primary auditory, temporal, hippocampus, primary

visual, occipital, basal ganglia, cerebellum, and white matter. The detailed methodology has been described previously (Yamaguchi *et al.*, 1997).

SPM

Basic image processing and voxel-based data analysis were performed using SPM2 (Wellcome Department of Cognitive Neurology, London, U.K.) on a Windows XP machine. PET data were subjected to an affine and non-linear spatial normalization into the standard MNI PET template of SPM2, and to re-slicing of 2×2×2 mm. The PET images were smoothed using an isotropic Gaussian filter of 12 mm in diameter to compensate for intersubject gyral variability and to reduce high-frequency noise. The anatomically standardized images were then normalized by ANCOVA to a mean value of 50 mg/100 g/min. The four groups (CDR 0, CDR 0.5/non-converters, CDR 0.5/converters, AD) were compared with ANCOVA (covariance of age and educational level). Pairs of groups were compared with unpaired t-tests. For multiple comparison, significance was accepted if the voxels survived an uncorrected threshold of $p < 0.001$.

INDIVIDUAL ANALYSIS

Individual CMRglc pattern analysis was conducted using the classification of Silverman *et al.* (2001): N1, normal metabolism; N2, global hypometabolism; N3, focal hypometabolism; P1, parietal/temporal with/without frontal hypometabolism; P2, frontal predominant hypometabolism; P3, hypometabolism of both the caudate head and lentiform nuclei. N indicates non-progressive PET patterns, and P shows progressive PET patterns. P1 indicates a PET pattern consistent with AD, and P2 and P3 indicate progressive but non-AD patterns. The patterns were compared between CDR 0.5/non-converters and CDR 0.5/converters by χ^2 test.

Clinical reassessments

In Incidence Study 2003, the CDR stages of all the subjects in the current PET study were reassessed to determine whether they met the criteria for dementia and AD. The reassessments were performed by evaluators who were blinded to the baseline CDR, neuropsychological tests, and PET findings. We mainly focused on CDR 0.5 subjects to determine whether they met the criteria for CDR 1 and AD.

Results

Clinical outcome

All participants in the CDR 0 group were reassessed as CDR 0 after the five-year period. In the CDR 0.5 group, 20 participants converted to AD (CDR 0.5/converters) and 22 participants remained as CDR 0.5 (CDR 0.5/non-converters). All AD patients declined to CDR 2. The demographics of the four groups are shown in Table 1. Age and educational level did not differ significantly among the groups. The AD group had significantly lower cognitive scores compared with the other groups.

Cognitive impairment

The CASI scores of the four groups are shown in Table 2. The AD group had significantly lower scores for all domains except "remote memory," compared with the other groups. CDR 0.5/converters showed a significantly lower "recent memory" score compared with CDR 0.5/non-converters.

Baseline glucose metabolism

Absolute rCMRglc values were calculated using arterial blood sampling and autoradiography. Using the ROI method, we found that the AD group had severely decreased rCMRglc compared with other groups, except in the basal ganglia and white matter, as shown in Table 3. There was no significant difference between CDR 0.5/non-converters and the CDR 0 group. However, CDR 0.5/converters had decreased rCMRglc in the temporoparieto-occipital (TPO) and hippocampus compared with CDR 0 subjects, and decreased rCMRglc in the TPO compared with CDR 0.5/non-converters.

SPM

COMPARISONS OF CDR 0.5 SUBJECTS WITH CDR 0 SUBJECTS AND AD PATIENTS

Comparisons of CDR 0.5/converters and CDR 0.5/non-converters with CDR 0 subjects are shown in Figure 1, and similar comparisons with AD

Table 1. Demographics of the study population at baseline

GROUP	MALE/FEMALE	AGE (y)	EDUCATION (y)	CASI TOTAL
CDR 0	4/10	77.7 (1.5)	8.4 (0.2)	89.7 (1.4)
CDR 0.5/non-converters	7/15	78.0 (1.6)	8.4 (0.2)	87.9 (1.6)
CDR 0.5/converters	7/13	78.4 (1.7)	9.1 (0.3)	79.9 (1.7)
AD	6/6	80.0 (1.8)	8.3 (0.4)	50.7 (2.4) [†]

Shown are the mean (SD).

Age (one-way ANOVA, $F = 2.410$, $p = 0.081$) and educational level ($F = 0.393$, $p = 0.0759$) did not differ significantly among the groups. The AD group had significantly lower cognitive scores compared with the other groups ($F = 35.810$, $p < 0.0001$)^(†).

CDR = Clinical Dementia Rating, AD = Alzheimer's disease.

CASI = Cognitive Abilities Screening Instrument.

Table 2. Cognitive performances of four groups at baseline

CASI ITEMS	CDR 0	CDR 0.5/ NON-CONVERTERS	CDR 0.5/ CONVERTERS	AD	F VALUE	p VALUE
Remote Memory	10.0 (0.0)	10.0 (0.0)	9.6 (0.8)	8.3 (2.9)	2.209	0.073
Recent Memory	10.8 (1.6)	10.8 (1.6)	6.8 (3.1) ^{a,b}	2.8 (1.9) ^{a,b,c}	20.900	0.000
Attention	6.5 (1.3)	6.8 (1.7)	6.9 (1.0)	4.4 (2.0) ^{b,c}	3.860	0.006
Concentration/ Mental Manipulation	7.3 (1.7)	7.6 (1.6)	7.5 (2.0)	3.8 (3.4) ^{a,b,c}	6.402	0.000
Orientation	17.8 (0.4)	16.7 (3.1)	15.2 (3.3)	5.3 (3.7) ^{a,b,c}	26.056	0.000
Visual Construction	9.9 (0.3)	9.7 (0.7)	9.7 (0.5)	7.7 (2.4) ^{a,b,c}	5.880	0.000
Abstraction and Judgement	9.2 (2.2)	8.8 (2.1)	6.9 (2.0)	5.1 (2.9) ^{a,h}	5.886	0.000
List-generating Fluency	8.0 (1.8)	7.6 (2.2)	6.5 (1.8)	4.3 (2.0) ^{a,b}	6.159	0.000
Language	9.8 (0.4)	9.9 (0.3)	9.7 (0.5)	8.2 (2.0) ^{a,b}	4.057	0.005

Shows are the mean (SD).

ANCOVA among four groups with the age and education level as covariance was performed.

The AD group had significantly lower scores for all domains except "remote memory," compared with the other groups (ANCOVA, covariance of age and educational level, $p = 0.008$). CDR 0.5/converters showed a significantly lower "recent memory" score compared with CDR 0.5/non-converters (ANCOVA, covariance of age and educational level, $p = 0.008$). post hoc tests, significantly ($p < 0.05$) different from Normal (a), CDR 0.5/non-converters (b), and CDR 0.5/converters (c).

CDR = Clinical Dementia Rating, AD = Alzheimer's disease.

Table 3. ROI values of four groups

ROI	CDR 0 NORMAL (n = 14)	CDR 0.5/NON- CONVERTERS (n = 22)	CDR 0.5/ CONVERTERS (n = 20)	CDR 1+AD (N = 12)	MS	F- VALUE	p- VALUE
Upper frontal	8.58 (1.17)	8.31 (0.43)	8.13 (0.38)	5.73 (0.86) ^{abc}	22.433	44.054	<0.001
Anterior frontal	7.64 (1.33)	7.09 (0.49)	6.90 (0.63)	4.64 (1.03) ^{abc}	22.522	30.436	<0.001
Inferior frontal	6.72 (1.31)	6.24 (0.51)	6.08 (0.42)	4.96 (0.90) ^{abc}	7.061	11.258	<0.001
Parietal	8.35 (1.13)	8.02 (0.42)	7.99 (0.47)	5.46 (0.83) ^{abc}	23.181	46.317	<0.001
TPO	7.31 (1.13)	6.87 (0.36)	5.84 (0.43) ^{ab}	4.34 (1.07) ^{abc}	23.774	43.005	<0.001
Primary auditory	8.81 (0.85)	8.59 (0.44)	8.54 (0.44)	5.16 (0.96) ^{abc}	39.814	93.525	<0.001
Temporal	6.89 (1.35)	6.42 (0.48)	6.26 (0.53)	4.50 (0.93) ^{abc}	14.053	20.761	<0.001
Hippocampus	6.20 (0.86)	6.05 (0.52)	5.45 (0.70) ^a	4.50 (0.95) ^{abc}	8.106	15.092	<0.001
Primary visual	9.34 (1.24)	8.43 (0.51)	8.19 (0.63)	5.70 (0.84) ^{abc}	29.721	24.293	<0.001
Occipital	7.91 (1.18)	7.11 (0.50)	6.54 (0.91)	4.16 (0.82) ^{abc}	42.626	52.311	<0.001
Basal ganglia	6.58 (1.16)	6.43 (0.27)	6.38 (0.30)	6.02 (0.76)	0.723	1.716	0.172
Cerebellum	7.32 (1.20)	7.39 (0.31)	7.27 (0.43)	6.06 (1.00) ^{abc}	5.371	9.721	<0.001
White matter	5.94 (1.08)	5.70 (0.32)	5.62 (0.52)	5.38 (0.88)	0.701	1.458	0.234

Shown are the means (SD).

The AD group had severely decreased rCMRglc compared with other groups, except in the basal ganglia and white matter (multiple ANOVAs and post hoc tests). There were no significant differences between CDR 0.5/non-converters and the CDR 0 group. However, CDR 0.5/Converters had decreased rCMRglc in the TPO and hippocampus compared with CDR 0 subjects, and decreased rCMRglc in the TPO compared with CDR 0.5/non-converters. post hoc tests, significantly ($p < 0.05$) different from Normal (a), CDR 0.5/non-converters (b), and CDR 0.5/converters (c). ROI = region of interests, TPO = Temporo-parieto-occipital, CDR = Clinical Dementia Rating, con. = converters, AD = Alzheimer's disease.

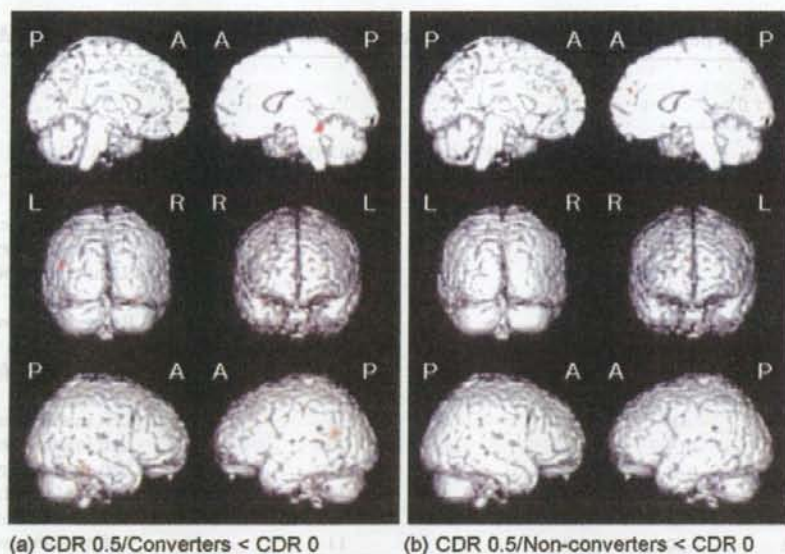


Figure 1. Results from voxel-based analysis with SPM2. (a) Voxels showing significant hypometabolism for CDR 0.5/converters compared to CDR 0 subjects ($p < 0.001$, uncorrected). (b) Voxels showing significant hypometabolism for CDR 0.5/non-converters compared to CDR 0 subjects ($p < 0.001$, uncorrected). The local maxima for the brain regions are shown in Table 3.

patients are shown in Figure 2. A region of hypometabolism was considered significant at $p < 0.001$ (uncorrected) for a cluster of ≥ 20 contiguous voxels superimposed on 3D-rendered MR images in Montreal Neurological Institute (MNI) space (Evans *et al.*, 1994). Brain areas reaching the

significance threshold were identified by voxel coordinates and labeled according to Talairach and Tournoux after coordinate conversion from MNI to Talairach space using a non-linear transformation algorithm (<http://imaging.mrc-cbu.cam.ac.uk/imaging/MniTalairach>) (Talairach and Tournoux,

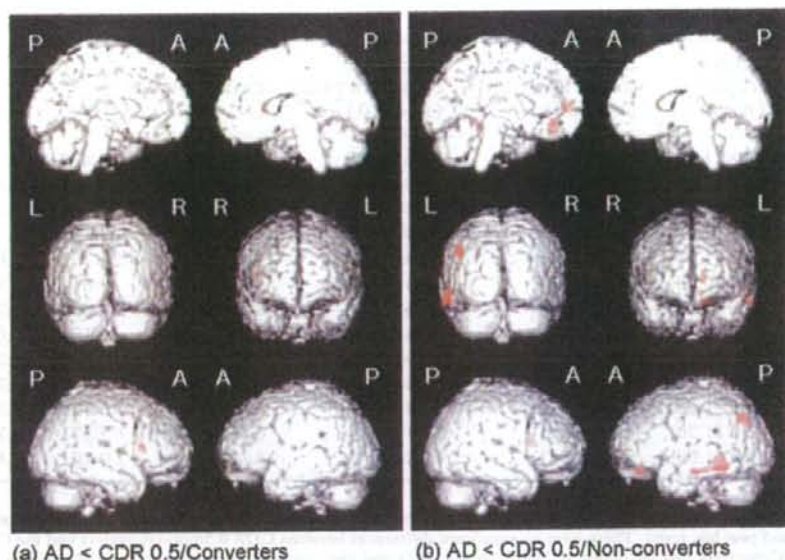


Figure 2. (a) Voxels showing significant hypometabolism for patients with AD compared to CDR 0.5/converters ($p < 0.001$, uncorrected). (b) Voxels showing significant hypometabolism for patients with AD compared to CDR 0.5/non-converters ($p < 0.001$, uncorrected).

Table 4. Location and peak coordinates of significant voxels from voxel-based analysis using SMP2

TALAIRACH COORDINATES			T STATISTICS	BRODMANN	ANATOMIC REGION
x	y	z			
<i>CDR 0.5/converters < CDR 0</i>					
-44	-53	19	4.04	22	Left superior temporal gyrus
-44	-46	17	3.57	22	Left superior temporal gyrus
36	-36	-13	4.01	36	Right parahippocampal gyrus
<i>CDR 0.5/con-converters < CDR 0</i>					
8	51	20	3.59	9	Right medial frontal gyrus
<i>AD < CDR 0.5/converters</i>					
44	20	10	4.04	45	Right inferior frontal gyrus
<i>AD < CDR 0.5/non-converters</i>					
-55	-45	-8	4.91	21	Left middle temporal gyrus
-57	-32	-15	3.77	20	Left inferior Temporal gyrus
-26	-45	-8	4.14	37	Left fusiform gyrus
46	18	10	4.08	45	Right inferior frontal gyrus
-10	57	5	3.97	10	Left medial frontal gyrus
-12	38	-20	3.70	11	Left straight gyrus
-5	34	-8	3.54	32	Left cingulate gyrus
-44	-71	35	3.37	39	Left angular gyrus
<i>CDR 0.5/converters < CDR 0.5/non-converters</i>					
-40	-61	25	3.85	39	Left middle temporal gyrus
-46	-40	22	3.61	40	Left inferior parietal lobule
12	-37	37	3.61	31	Right cingulate gyrus
-55	-43	-11	3.51	37	Left inferior temporal gyrus

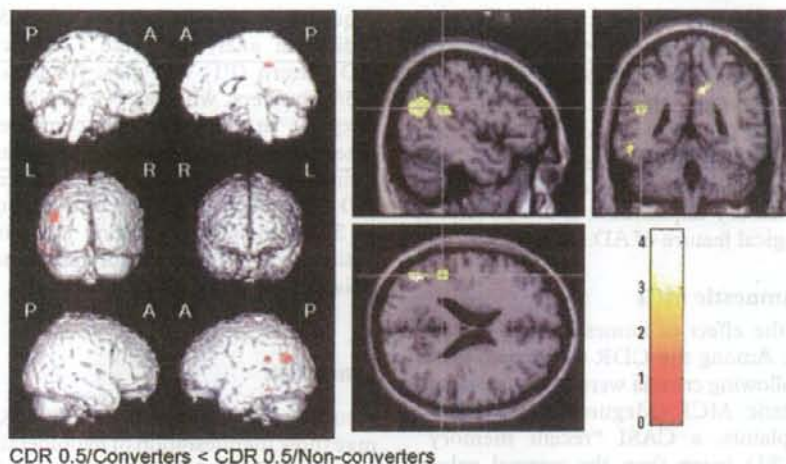


Figure 3. (Left) Voxels showing significant hypometabolism for CDR 0.5/converters compared to CDR 0.5/non-converters ($p < 0.001$, uncorrected). (Right) The same results were displayed on 2D planes of a normal MRI template provided by SPM2 to clarify their anatomic locations. The color bar represents t values derived from the voxel-based analysis.

Table 5. PET patterns of Silverman's classification for two CDR 0.5 groups

	N1	N2	N3	P1	P2	P3	TOTAL
Non-converters	5	5	7	5	0	0	23
Converters	3	1	4	12	0	0	20

N = non-progressive patterns, p = progressive patterns

1998). Areas showing a significant difference (SPM2, $p < 0.001$, uncorrected) are shown in Table 4. For multiple comparisons, the significance level was set at 0.001.

COMPARISON BETWEEN CDR 0.5/CONVERTERS AND CDR 0.5/NON-CONVERTERS

CDR 0.5/converters had significantly lower CMRglc values (SPM2, $p < 0.001$, uncorrected) in the left middle temporal gyrus, left inferior parietal lobule, right cingulate gyrus, and left inferior temporal gyrus, compared with CDR 0.5/non-converters (Figure 3 and see Table 4).

INDIVIDUAL ANALYSIS USING SILVERMAN'S CLASSIFICATION

PET patterns using Silverman's classification for the two CDR 0.5 groups are shown in Table 5. The difference between the groups was significant by χ^2 test ($p < 0.05$), with CDR 0.5/converters showing a P1 pattern more frequently. No participants showed P2 or P3 patterns. Comparing all non-progressive patterns (N1–N3) with the progressive pattern (P1) for the two groups, a true positive rate (sensitivity) of 0.60, a true negative rate (specificity) of 0.74, a positive predictive value of 0.71, and a negative

predictive value of 0.68 were found. Of the 14 normal subjects, 12 showed an N1 pattern and 2 had an N2 pattern. The 12 AD patients all showed P1 patterns.

Discussion

In this study, CDR 0.5/converters showed greater baseline hypometabolism compared with CDR 0.5/non-converters in brain areas specific for AD, suggesting that CDR 0.5 converters might have AD-like changes.

Methodological issues

There are some methodological limitations in the study. First, only 40% of the CDR 0 subjects and 70% of the CDR 0.5 subjects were scanned due to limited availability of the FDG-PET scanner (an average of four patients a month). The long distance between Tajiri and the PET center also prevented some older adults from participating in the study. Therefore, there may be some sampling bias and caution is required in interpretation of the results. Second, evaluation was only performed at two time points, rather than annually; however, the administrative situation brought about by the formation of a new city in 2006 through the merger of several towns, including Tajiri, prevented use of an annual study design. Third, although the CASI provided sufficient information for a detailed analysis, assessments such as the WMS-R for memory and the WAIS-R for general intelligence would have provided more cognitive information; however, the time required for assessing community residents prevented use of these tests.

Neuropsychological findings

Only the CASI "recent memory" score showed a significant difference between CDR 0.5/converters and CDR 0.5/non-converters ($p = 0.008$). This is consistent with previous studies (Arnaiz *et al.*, 2001; Visser *et al.*, 2002) and suggests that CDR 0.5/converters already have AD-like changes, since recent memory impairment is a well-known neuropsychological feature of AD.

Criteria for amnesic MCI

We evaluated the effect of amnesic MCI criteria retrospectively. Among the CDR 0.5 group, those who met the following criteria were also considered to have amnesic MCI (Meguro *et al.*, 2004): memory complaints, a CASI "recent memory" score of -1.5 SD lower than the normal values for each age group, and normal MMSE scores for each educational level. Four CDR 0.5 subjects met these criteria and all converted to AD. Although the sample size was small, these results suggest that criteria for amnesic MCI are more "specific" for AD changes, whereas CDR 0.5 criteria are more "sensitive."

Metabolic patterns of CDR 0.5 converters

The lack of metabolic differences after taking CASI scores into covariance might indicate that cognitive, rather than metabolic, differences predict conversion to AD. However, the aim of this study was to investigate whether metabolic changes in CDR 0.5 converters manifest as a decrease in CMRglc in a manner specific to early AD. Although the predictive power may be stronger for cognitive dysfunction, we believe that the findings support the hypothesis of the study.

Our findings suggest that CDR 0.5 participants who decline to AD develop hypometabolism in the posterior cingulate and other brain regions that might be specific to AD. These hypometabolic areas are similar to those observed in patients with probable AD (Hoffman *et al.*, 2000). Previous longitudinal studies on amnesic MCI have also indicated that these areas differ significantly between converters and non-converters (Arnaiz *et al.*, 2001; Chetelat *et al.*, 2003; Drzezga *et al.*, 2003; Mosconi *et al.*, 2004). A follow-up SPECT study on amnesic MCI also showed asymmetric reduction of perfusion in the parahippocampus, lateral parietal lobe, and posterior cingulate cortices in converters (Ishiwata *et al.*, 2006). Parahippocampal gyri are very small areas and other studies may have missed these regions using the SPM method.

Since SPM reveals much more restricted abnormalities than suggested by individual classification, analysis of the individual patterns is

required to provide support for SPM findings. In individual analysis of the CMRglc pattern, the AD pattern (P1) was most frequent among CDR 0.5/converters, whereas N1 and N3 patterns were frequent in CDR 0.5/non-converters (Table 5). These results are consistent with past studies and indicate that most CDR 0.5/converters already have AD pathology. The data also support the results of SPM analysis, indicating that both visual and automated methods are preferable to confirm the reliability of acquired data.

Conclusion

Neurological findings for MCI/CDR 0.5 decliners may show manifestation of hypometabolism in brain areas specific to AD. Since the prevalence of CDR 0.5 is much higher than that of MCI and the rate of decline to dementia from the two conditions is about the same, use of CDR 0.5 criteria may increase the detection rate of decliners in a community population.

Conflict of interest

None.

Description of authors' roles

K. Meguro and H. Ishii designed the study, supervised the data collection and wrote the paper. K. Meguro and S. Yamaguchi collected the data. H. Ishikawa and M. Tashiro were responsible for the statistical design of the study and for statistical analysis.

Acknowledgments

We are grateful to the town officials of Tajiri. This study was supported in part by a JST grant for research and education in molecular imaging.

References

- American Psychiatric Association (1994). *Diagnostic and Statistical Manual of Mental Disorders*, 4th edn. Washington, DC: American Psychiatric Association.
- Arnaiz, E. *et al.* (2001). Impaired cerebral glucose metabolism and cognitive functioning predict deterioration in mild cognitive impairment. *NeuroReport*, 12, 851-855.
- Chen, P., Ratcliff, G., Belle, S. H., Cauley, J. A., DeKosky, S. T., and Ganguli, M. (2000). Cognitive tests that best discriminate between presymptomatic AD and

- those who remain nondemented. *Neurology*, 55, 1847–1853.
- Chetelat, G., Desgranges, B., de la Sayette, V., Viader, F., Eustache, F. and Baron, J. C.** (2003). Mild cognitive impairment: can FDG-PET predict who is to rapidly convert to Alzheimer's disease? *Neurology*, 60, 1374–1377.
- Drzezza, A. et al.** (2003). Cerebral metabolic changes accompanying conversion of mild cognitive impairment into Alzheimer's disease: a PET follow-up study. *European Journal of Nuclear Medicine and Molecular Imaging*, 30, 1104–1113.
- Evans, A. D. et al.** (1994). 3D statistical neuroanatomical models from 305 MRI volumes. *IEEE Nuclear Science Symposium Medical Imaging Conference*, 3, 1813–1817.
- Fellgiebel, A., Scheurich, A., Bartenstein, P. and Muller, M. J.** (2007). FDG-PET and CSF phospho-tau for prediction of cognitive decline in mild cognitive impairment. *Psychiatry Research*, 155, 167–171.
- Folstein, M. F., Folstein, S. E. and McHugh, P. R.** (1975). "Mini-mental state": a practical method for grading the cognitive state of patients for the clinician. *Journal of Psychiatric Research*, 12, 189–198.
- Hoffman, J. M. et al.** (2000). FDG PET imaging in patients with pathologically verified dementia. *Journal of Nuclear Medicine*, 41, 1920–1928.
- Ishiwata, A., Sakayori, O., Minoshima, S., Mizumura, S., Kitamura, S. and Katayama, Y.** (2006). Preclinical evidence of Alzheimer changes in progressive mild cognitive impairment: a qualitative and quantitative SPECT study. *Acta Neurologica Scandinavica*, 114, 91–96.
- Larrieu, S. et al.** (2002). Incidence and outcome of mild cognitive impairment in a population-based prospective cohort. *Neurology*, 59, 1594–1599.
- McKhann, G., Drachman, D., Folstein, M., Katzman, R., Price, D. and Stadlan, E. M.** (1984). Clinical diagnosis of AD: report of the NINCDS-ADRDA work group under the auspices of department of health and human services task force on AD. *Neurology*, 34, 939–944.
- Meguro, K.** (2004). *A Clinical Approach to Dementia: An Instruction of CDR Worksheet*. Tokyo: Igaku-Shoin.
- Meguro, K. et al.** (2002). Prevalence of dementia and dementing diseases in Japan: the Tajiri Project. *Archives of Neurology*, 59, 1109–1114.
- Meguro, K. et al.** (2004). Prevalence and cognitive performances of Clinical Dementia Rating 0.5 and mild cognitive impairment in Japan: the Tajiri Project. *Alzheimer Disease and Associate Disorders*, 18, 3–10.
- Meguro, K. et al.** (2007). Incidence of dementia and associated risk factors in Japan: The Osaki-Tajiri Project. *Journal of Neurological Sciences*, 260, 175–182.
- Morris, J. C.** (1993). The Clinical Dementia Rating (CDR): current version and scoring rules. *Neurology*, 43, 2412–2414.
- Morris, J. C. et al.** (2001). Mild cognitive impairment represents early-stage Alzheimer's disease. *Archives of Neurology*, 58, 397–405.
- Mosconi, L. et al.** (2004). MCI conversion to dementia and the APOE genotype: a prediction study with FDG-PET. *Neurology*, 63, 2332–2340.
- Pernecky, R., Hartmann, J., Grimmer, T., Drzezza, A. and Kurz, A.** (2007). Cerebral metabolic correlates of the Clinical Dementia Rating scale in mild cognitive impairment. *Journal of Geriatric Psychiatry and Neurology*, 20, 84–88.
- Petersen, R. C., Smith, G. E., Waring, S. C., Ivnik, R. J., Kokmen, E. and Tangalos, E. G.** (1997). Aging, memory, and mild cognitive impairment. *International Psychogeriatrics*, 9, 65–69.
- Phelps, M. E., Huang, S. C., Hoffman, E. J., Selin, C., Sokoloff, L. and Kuhl, D. E.** (1979). Tomographic measurement of local glucose metabolic rate in humans with (FO-18)2-fluoro-2-deoxy-D-glucose: validation of method. *Annals of Neurology*, 6, 371–388.
- Reisberg, B., Ferris, S. H. and de Leon, M. J.** (1982). The global deterioration scale for assessment of primary degenerative dementia. *American Journal of Psychiatry*, 139, 1136–1139.
- Reivich, M. et al.** (1979). The ¹⁸F-fluoro-deoxyglucose method for the measurement of local cerebral glucose utilization in man. *Circulation Research*, 44, 127–137.
- Silverman, D. H. et al.** (2001). Positron emission tomography in evaluation of dementia: regional brain metabolism and long-term outcome. *JAMA*, 286, 2120–2127.
- Talairach, J. and Tournoux, P.** (1988). *Co-planar Stereotaxic Atlas of the Human Brain: 3-dimensional Proportional System: An Approach to Cerebral Imaging*. New York: Thieme Medical.
- Teng, E. L. et al.** (1994). The Cognitive Ability Screening Instrument (CASI): a practical test for cross-cultural epidemiological studies of dementia. *International Psychogeriatrics*, 6, 45–58.
- Visser, P. J., Verhey, F. R., Hofman, P. A., Scheltens, P. and Jolles, J.** (2002). Medial temporal lobe atrophy predicts Alzheimer's disease in patients with minor cognitive impairment. *Journal of Neurology, Neurosurgery, and Psychiatry*, 72, 491–497.
- Yamaguchi, S. et al.** (1997). Decreased cortical glucose metabolism correlated with hippocampal atrophy in Alzheimer's disease as shown by MRI and PET. *Journal of Neurology, Neurosurgery, and Psychiatry*, 62, 596–600.

In vivo visualization of donepezil binding in the brain of patients with Alzheimer's disease

Nobuyuki Okamura,¹ Yoshihito Funaki,² Manabu Tashiro,³
Motohisa Kato,¹ Yoichi Ishikawa,² Masahiro Maruyama,⁴
Hiroyasu Ishikawa,⁵ Kenichi Meguro,⁵ Ren Iwata² & Kazuhiko Yanai¹

¹Department of Pharmacology, Tohoku University Graduate School of Medicine, Sendai, ²Division of Radiopharmaceutical Chemistry, Cyclotron and Radioisotope Center, Tohoku University, Sendai,

³Division of Nuclear Medicine, Cyclotron and radioisotope centre, Tohoku University, Sendai,

⁴Department of Geriatric and Complementary Medicine, Tohoku University Graduate School of Medicine, Sendai and ⁵Department of Geriatric Behavioural Neurology, Tohoku University Graduate School of Medicine, Sendai, Japan

WHAT IS ALREADY KNOWN ABOUT THIS SUBJECT

- Deficit in central cholinergic neurotransmission is a consistent change associated with Alzheimer's disease (AD).
- Donepezil hydrochloride exhibits selective inhibition of acetylcholinesterase (AChE) and is widely used for the treatment of AD.
- The biodistribution of donepezil in the brain after administration is not precisely understood *in vivo*.
- There is no method to measure the amount of binding of orally administered donepezil to AChE.

WHAT THIS STUDY ADDS

- This study clearly visualizes the distribution of donepezil in human brain using [¹¹C]-donepezil and positron emission tomography.
- This study demonstrates prominent reduction of the donepezil binding site in the AD brain.
- This study provides methodology to measure the AChE binding occupancy of orally administered donepezil and provides a new surrogate marker for evaluation and prediction of response to donepezil treatment.

Correspondence

Dr Nobuyuki Okamura MD, PhD,
Department of Pharmacology, Tohoku
University School of Medicine, 2-1,
Seiryō-machi, Aoba-ku, Sendai 980-8575,
Japan.
Tel: +81 2 2717 8058;
Fax: +81 2 2717 8060;
E-mail: oka@mail.tains.tohoku.ac.jp

Keywords

acetylcholinesterase, Alzheimer's disease,
donepezil, positron emission tomography
(PET)

Received

1 July 2007

Accepted

26 September 2007

Published Online Early

7 December 2007

AIMS

The aims of this study were to visualize *in vivo* binding of donepezil to acetylcholinesterase (AChE) in the brain and to establish a method for measuring the amount of binding of orally administered donepezil.

METHODS

[5-¹¹C-methoxy]-donepezil ([¹¹C]-donepezil) was radiolabelled as a positron emission tomography (PET) tracer. The biodistribution of [¹¹C]-donepezil was measured by PET in 10 AD patients and six elderly normal subjects. Two AD patients underwent additional PET measurements after oral administration of donepezil for 6 months.

RESULTS

[¹¹C]-donepezil-PET images demonstrated high densities of tracer distribution in AChE-rich brain regions such as the striatum, thalamus, and cerebellum. Compared with elderly normal subjects, patients with mild AD exhibited about 18–20% reduction of donepezil binding in the neocortex and hippocampus, while patients with moderate AD exhibited about 24–30% reduction of donepezil binding throughout the brain. Orally administered donepezil (5 mg day⁻¹) induced 61.6–63.3% reduction of donepezil binding in AD brains. The distribution volume of [¹¹C]-donepezil in the hippocampus was significantly correlated with MMSE scores in AD patients.

CONCLUSIONS

[¹¹C]-donepezil-PET enables quantitative measurement of donepezil binding in the brain. AD patients exhibited reduction of donepezil binding in the brain, even in the early stage of disease. Longitudinal evaluation by this technique enables determination of AChE binding occupancy of orally administered donepezil.

Introduction

Cholinergic deficit is consistently found in the brain of patients with Alzheimer's disease (AD). Reduction in the activity of choline acetyltransferase (ChAT) and acetylcholinesterase (AChE) is evident in AD brains and correlates with cognitive decline [1, 2]. For this reason, cholinergic enhancement is a major approach to the treatment of AD. Currently, several AChE inhibitors (AChEIs) are widely prescribed to improve cognitive function in patients with AD [3]. However, not all patients respond to these treatments. It is thus important to identify factors that determine individual responses to treatment with AChEIs.

Functional imaging of cholinergic function is a useful strategy for determination of the treatment protocol of demented patients. Use of AChEIs themselves as radiotracers enables direct investigation of the pharmacokinetics of AChEIs using positron emission tomography (PET). Donepezil hydrochloride is currently the AChEI most widely used for the treatment of AD. It exhibits selective binding of AChE compared with butyrylcholinesterase (BuChE) [4]. Radiolabelled donepezil can thus be used as a tracer to measure brain concentrations of AChE. If the distribution of donepezil in the brain can be measured quantitatively by PET, this will be useful for pharmacological evaluation of AChEIs and for prediction of efficacy of treatment with donepezil. In this study, we performed PET examinations using [5-¹¹C-methoxy]-donepezil ([¹¹C]-donepezil) and determined the *in vivo* binding characteristics of donepezil in AD patients.

Methods

Subjects and patients

Six elderly normal subjects and 10 patients with probable AD were studied to examine the distribution of [¹¹C]-donepezil in the brain. The AD patients were recruited through The Tohoku University Hospital Dementia Patients Registry. The diagnosis of AD was made according to the National Institute of Neurologic Disorders and Stroke/Alzheimer's Disease and Related Disorders Association (NINCDS-ADRDA) criteria. AD patients were further divided into two groups by severity: a mild AD group ($n = 5$; MMSE score ≥ 23 points) and a moderate AD group ($n = 5$; MMSE score < 20 points). The normal control group was comprised of volunteers without impairment of cognitive function who had no cerebrovascular lesions on magnetic resonance (MR) images. After complete description of the study to the patients and subjects, written informed consent was obtained from them. PET study was performed within 3 months after the completion of a medical and neuropsychological examination. Although no significant difference in age was observed between the mild AD group and elderly normal group, the moderate AD group was older than the elderly normal group (Table 1). The

Table 1

Subjects and patients demographics

		Gender	Age	MMSE
Elderly normal	AN1	M	64	30
	AN2	M	61	30
	AN3	F	59	30
	AN4	F	60	30
	AN5	M	74	28
	AN6	F	75	30
	Mean		65.5	29.7
	SD		7.2	0.8
Mild AD	AD1	F	77	24
	AD2	F	72	23
	AD3	M	71	26
	AD4	F	66	25
	AD5	M	69	27
	Mean		71.0	25.0
	SD		4.1	1.6
Moderate AD	AD6	F	77	14
	AD7	F	78	12
	AD8	F	79	19
	AD9	M	84	17
	AD10	F	81	15
	Mean		79.8	15.4
		SD		2.8

MMSE score of the elderly normal subjects (mean \pm SD 29.7 ± 0.8) was significantly higher than that of the mild AD (25.0 ± 1.6) and moderate AD (15.4 ± 2.7) subjects.

Radiosynthesis of [5-¹¹C-methoxy]-donepezil

Synthesis of [¹¹C]-donepezil was performed (Figure 1) as described previously [5]. Briefly, 5'-O-desmethylprecursor (M2) was dissolved in methylethylketone and then tetrabutylammonium hydroxide was added. [¹¹C]-Methyl iodide was prepared from [¹¹C]-CO₂ and converted to [¹¹C]-methyl triflate ([¹¹C]-MeOTf). [¹¹C]-Donepezil was produced on the loop from [¹¹C]-MeOTf and purified by high performance liquid chromatography (HPLC). The radioactivity obtained was 155.4–814 MBq (4.2–22 mCi), and the radiochemical yield was 25–30% based on [¹¹C]-MeOTf after decay-correction. Specific activity was 111–354 GBq μmol^{-1} at the end of synthesis (30–40 min from the end of ¹¹C production). Radiochemical purity was greater than 99%.

PET acquisition protocols

The protocol of the PET study was approved by the Committee on Clinical Investigation at The Tohoku University School of Medicine and the Advisory Committee on Radioactive Substances at Tohoku University. The [¹¹C]-donepezil PET study was performed using a SET-2400 W PET scanner (Shimadzu Inc., Japan) under resting condition with eyes closed. Following a ⁶⁸Ge/Ga transmission scan of 7 min duration, an emission scan was started soon after intravenous injection of 7.1–9.5 mCi of [¹¹C]-donepezil. Emission

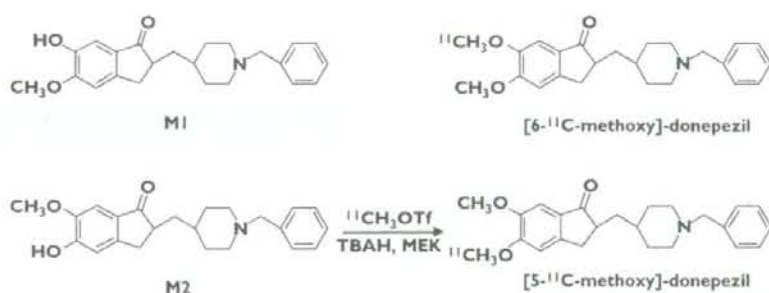


Figure 1

Chemical structures and radiosynthesis of donepezil and its metabolites

data were acquired for 60 min. Standardized uptake value (SUV) images were obtained by normalizing tissue concentration by injected dose and body mass. Arterialized venous blood samples were obtained from a hand vein, heated in a far-infrared mat, and radioactivity was measured in a well-type scintillation counter. Sampled plasma (2 ml) was denatured with 1 M HClO₄:MeCN (7:3) and centrifuged at 3000 × g for 3 min. The supernatant solution was injected into a column (YMC ODS A-324, YMC Co., Ltd, Kyoto, Japan; 10 mm i.d. × 30 cm long) with a solvent system of 0.1 M ammonium formate:acetonitrile (60:40) at a flow rate of 5.0 ml min⁻¹. The eluates were collected at time intervals of 0.5 min and were counted for radioactivity with a gamma counter.

Image analysis

Region of interest (ROI) analysis was performed to evaluate the regional distribution of [¹¹C]-donepezil. Circular ROIs (1.0 cm in diameter) were placed on individual axial PET images in the cerebellar hemisphere, striatum, thalamus, lateral frontal cortex (Brodmann's areas (BA) 44, 45, 46, and 47), lateral temporal cortex (BA 20, 21, and 22), parietal cortex (BA 39 and 40), occipital cortex (BA 17), anterior cingulate cortex (BA 24 and 32), posterior cingulate cortex (BA 23 and 31), and medial temporal cortex (BA 27, 28, 34, and 35), referring to the individual MR images. To measure donepezil-binding AChE density in the brain, the distribution volume (DV), the ratio of [¹¹C]-donepezil concentration in tissue to that in plasma at equilibrium, was calculated by Logan's graphical analysis [6], since donepezil reversibly binds to AChE. Using this method, the DV in each ROI was determined from the slopes obtained from the values of each ROI and input function from metabolite-corrected plasma radioactivity. The slopes were determined from the last 15 points of the respective regions. Details of the quantitative analysis will be described elsewhere.

Statistical analysis

Differences in age, MMSE score, and DV among the three groups were evaluated by one-way analysis of variance

(ANOVA) followed by Bonferroni's multiple comparison test (GraphPad Prism Software). For each analysis, findings were considered significant at $P < 0.05$.

Results

Tissue time activity curves (TAC) of [¹¹C]-donepezil in the brain indicated initial rapid uptake of radioactivity followed by gradual clearance from the brain in both elderly normal (Figure 2A) and AD subjects (Figure 2B). Relatively high concentrations of radioactivity of [¹¹C]-donepezil were observed in AChE-rich brain regions such as the striatum, thalamus, and cerebellum, whereas radioactivity uptake in the neocortex including frontal, temporal, and parietal cortices was moderate. Plasma radioactivity of [¹¹C]-donepezil peaked at 30–60 s postinjection, followed by a rapid decline (Figure 2C). Proportions of unchanged [¹¹C]-donepezil in plasma were 91.0 ± 7.0%, 88.1 ± 12.5%, and 82.5 ± 5.1% at 5, 15, and 30 min postinjection, respectively. The metabolite-corrected plasma time-activity curve was used to calculate specific DVs from the region-of-interest-derived regional time-activity curve. [¹¹C]-donepezil exhibited linear regression curves on Logan plot analysis in all brain regions examined (Figure 3). Since the slopes of the regression lines represent the DV of the tracer, these findings indicate a higher DV of donepezil in the striatum than in the frontal cortex. Parametric images of [¹¹C]-donepezil DV clearly revealed higher concentrations of tracer distribution in the striatum and cerebellum than in the neocortex. Patients with mild AD exhibited reduction of DV in the hippocampus and neocortex, compared with elderly normal subjects. The magnitude of DV reduction in the mild AD group was about 20% in the hippocampus and 18% in temporal and parietal cortices. In patients with moderate AD, DV reduction was evident throughout the brain (Figure 4, Figure 5, Table 2). The magnitude of DV reduction was about 30% in the hippocampus and 24% in frontal, temporal, and parietal cortices. Two AD patients (AD3 and AD10) underwent another PET scan after treatment with 5 mg donepezil for 6 months. Orally

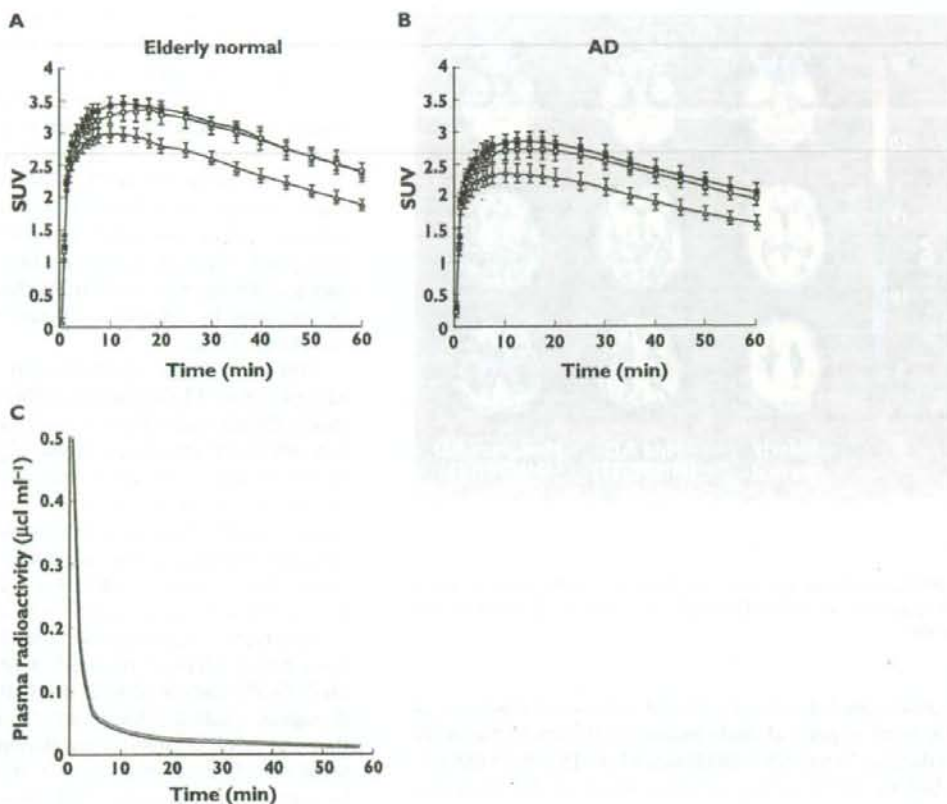


Figure 2

Time activity data for [^{11}C]-donepezil PET in humans. Brain SUV time activity curves for elderly normal subjects (A) and AD patients (B), and plasma time activity curve (C) are shown. The dotted line indicates total time activity curve and the solid line indicates metabolite-corrected time activity curve

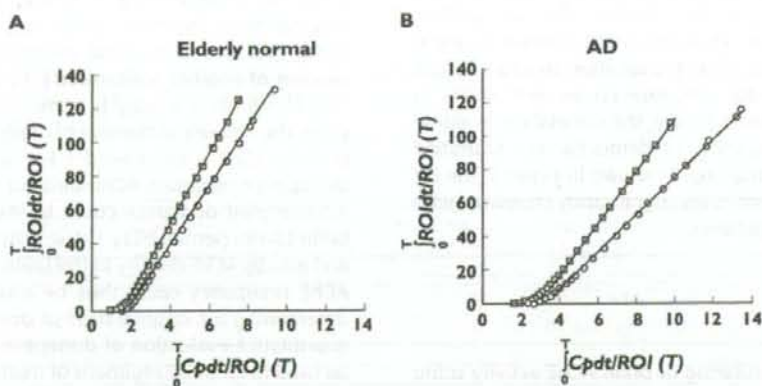


Figure 3

Logan plots for the striatum (\square) and frontal cortex (\circ) for elderly normal subjects (A) and AD patients (B). Cp: plasma concentration of tracer, ROI: region of interest, T: time after injection

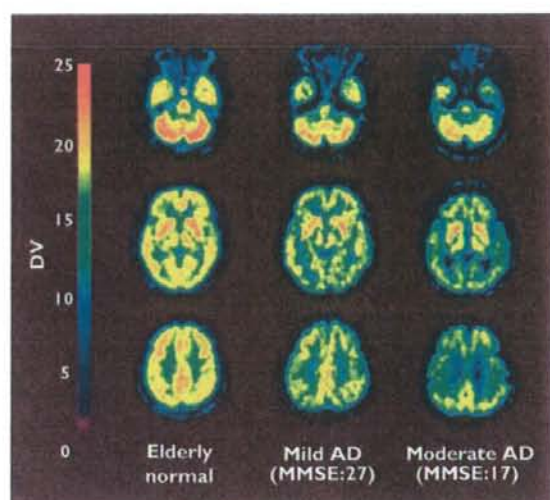


Figure 4

Distribution volume images of [¹¹C]-donepezil in elderly normal subjects (left), patients with mild AD (middle), and patients with moderate AD (right)

administered donepezil induced substantial reduction of DV in all regions of brain examined (Figure 6). Mean DV reduction in patient 1 (AD3) was 61.6% (55.5% in the cerebellum, 65.2% in the striatum, 63.6% in the thalamus, 62.5% in the frontal cortex, 61.6% in the temporal cortex, 59.6% in the parietal cortex, 62.6% in the occipital cortex, 60.3% in the anterior cingulate cortex, 59.5% in the posterior cingulate cortex and 65.5% in the medial temporal cortex). Mean DV reduction in patient 2 (AD10) was 63.3% (59.9% in the cerebellum, 72.0% in the striatum, 60.6% in the thalamus, 61.6% in the frontal cortex, 62.9% in the temporal cortex, 62.4% in the parietal cortex, 54.2% in the occipital cortex, 62.4% in the anterior cingulate cortex, 57.9% in the posterior cingulate cortex and 78.8% in medial temporal cortex). Finally, the correlation of donepezil binding with severity of dementia was examined within the AD patient group. As shown in Figure 7, the DV value in the hippocampus was significantly correlated with MMSE scores of AD patients.

Discussion

Currently, *in vivo* monitoring of brain AChE activity using positron emission tomography (PET) is beneficial in developing strategies for dementia therapy. [¹¹C]-MP4A and [¹¹C]-PMP, which are metabolically trapped acetylcholine analogues, have been successfully applied to the evaluation of AChE activity in the brain [7, 8]. PET studies in AD patients have demonstrated reduction of AChE activity in

the early stage of disease, with the degree of reduction correlating with cognitive dysfunction [9, 10]. Another strategy involves use of AChEIs themselves as radiotracers. This method enables direct investigation of the pharmacokinetics of AChEIs. [¹¹C]-physostigmine [11], [¹¹C]-methyltacrine [12], and [¹¹C]-CP-126 998 [13] have been designed as radiotracers for clinical PET study. *In vivo* imaging techniques using such radiotracers can measure the concentrations of tracer-binding AChE. If these radiotracers and therapeutic drugs competitively bind to AChE, the occupancy of binding sites on AChE by therapeutic drugs could be measured by subtraction of post-treatment from pre-treatment PET scans.

This PET study demonstrated that intravenously administered [¹¹C]-donepezil rapidly enters the brain and is mainly distributed in the striatum, thalamus, and cerebellum, which are known to contain high densities of AChE compared with the cerebral cortex and hippocampus. This finding is consistent with the findings of our previous study in rats [5]. The regional distribution of [¹¹C]-donepezil was also consistent with regional AChE activity determined in a human postmortem study [14], suggesting selective binding of donepezil to AChE.

Post-treatment evaluation following administration of 5 mg donepezil day⁻¹ revealed a remarkable reduction (61.6–63.3% compared with pretreatment scan) of [¹¹C]-donepezil binding throughout the brain. This indicates that the AChE occupancy by donepezil, when administered in daily doses of 5 mg, was about 35–40% in these two patients. A previous PET study using [¹¹C]-MP4A revealed a mean 39% reduction in AChE activity after oral administration of 3–5 mg donepezil [15]. Intravenous administration of donepezil in monkeys also resulted in a mean 27% reduction of AChE activity at a dose of 100 µg kg⁻¹ [16]. These findings together suggest that inhibition of AChE activity matches occupancy of AChE binding sites. Moreover, orally administered donepezil (5 mg) induced substantial inhibition (43–62%) of the binding of another radiotracer, [¹¹C]-CP-126 998, to AChE [13]. This finding is roughly consistent with our observations. The amount of binding of orally administered donepezil to AChE is considered a key factor in determining therapeutic response. AChE binding occupancy by orally administered donepezil could be modulated by blood-brain barrier permeability, tissue distribution, metabolism, and also by AChE density in the brain. *In vivo* evaluation of AChE occupancy could thus be a powerful strategy for determining the optimal dose of donepezil. In the future, quantitative evaluation of donepezil binding sites might be used to optimize regimens of treatment with donepezil and to predict the response to treatment. To this purpose, red blood cell AChE inhibition has been explored as a peripheral surrogate marker for the activity of AChEIs [17]. In a future study, we plan to examine the relationship between red blood cell AChE inhibition and [¹¹C]-donepezil binding in the brain.

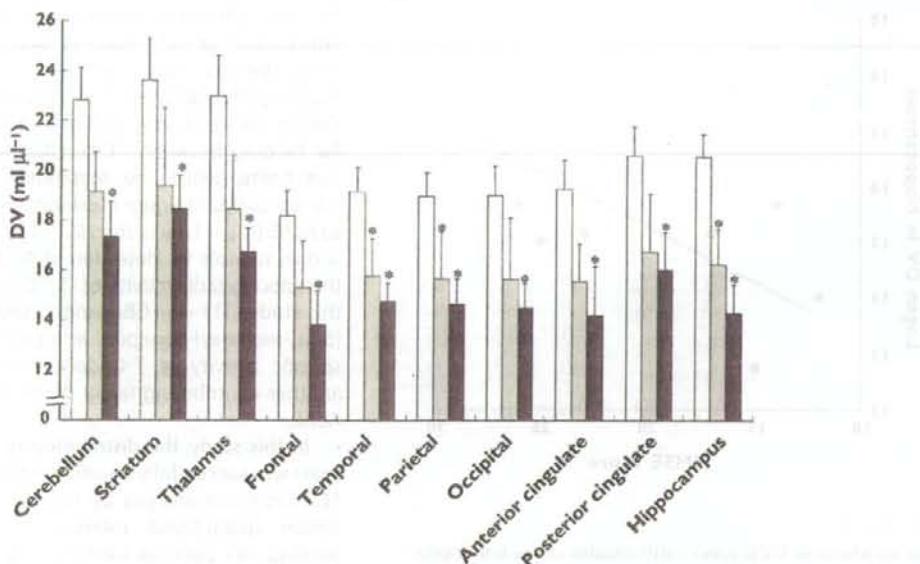


Figure 5

Regional distribution volume data in elderly normal subjects (□), mild AD (▒), and moderate AD patients (■)

Table 2

Regional distribution volume of [¹¹C]-donepezil in elderly normal subjects and AD patients (mean ± SEM)

	Elderly normal	Mild AD	Moderate AD
Cerebellum	23.4 ± 3.5	19.6 ± 1.4	17.6 ± 1.4*
Striatum	24.0 ± 4.1	20.0 ± 3.1	18.5 ± 1.6*
Thalamus	23.4 ± 4.1	19.0 ± 2.1	17.1 ± 1.0*
Frontal	18.5 ± 2.5	15.8 ± 1.8	14.0 ± 1.5*
Temporal	19.7 ± 2.6	16.2 ± 1.3*	15.1 ± 0.9*
Parietal	19.5 ± 2.7	16.1 ± 1.7*	15.0 ± 1.1*
Occipital	19.4 ± 3.2	16.1 ± 2.3	14.6 ± 1.1*
Anterior cingulate	19.6 ± 2.6	16.2 ± 1.7	14.7 ± 1.9*
Posterior cingulate	21.1 ± 3.0	17.2 ± 2.3	16.3 ± 1.7*
Hippocampus	21.4 ± 2.1	17.3 ± 2.1*	14.8 ± 1.2*

*P < 0.05, significantly different from aged normal group.

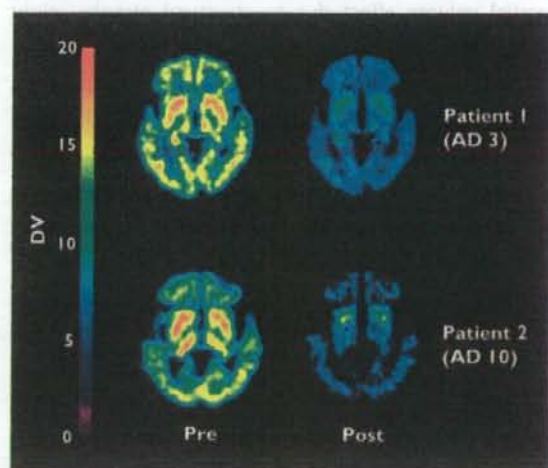


Figure 6

Distribution volume images before and after oral administration of donepezil in AD patients

mild AD group and 30% reduction in the moderate AD group. These findings suggest that the concentration of donepezil-binding AChE is matched by regional AChE activity. In a postmortem study, AD patients exhibited reduction of AChE activity, and this reduction was correlated with the severity of dementia [20, 21]. We observed

Patients with moderate AD exhibited significant reduction of [¹¹C]-donepezil DV in all brain regions examined, in comparison with elderly normal subjects. Furthermore, temporo-parietal and hippocampal DVs were significantly reduced even in patients with mild AD, compared with elderly normal group. These reductions suggest early involvement of the cholinergic system in AD, since the AChE in brain is predominantly located in presynaptic cholinergic neurones [18]. A previous [¹¹C]-MP4A PET study demonstrated 21% reduction of hippocampal AChE activity in patients with early onset AD [19]. We observed an approximately 20% reduction in hippocampal DV in the

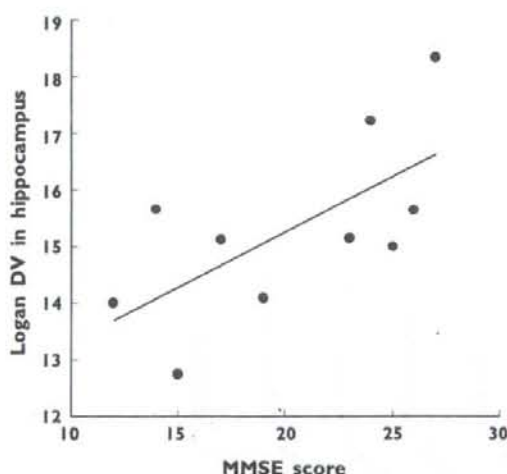


Figure 7

Correlation between MMSE scores and distribution volume in the hippocampus of AD patients. Pearson $r = 0.659$ and $p = 0.038$

that DV in the hippocampus was correlated with the cognitive status in AD patients, a finding in accord with post-mortem data. However, it is important to note that the partial volume effect due to structural atrophy might cause the underestimation of DV in the hippocampus. Analysis after partial volume correction is therefore needed to establish further the relationship between the regional DV of [^{11}C]-donepezil and the severity of dementia in AD.

Compared with previously reported findings of PET imaging with [^{11}C]-MP4A [9] and [^{11}C]-PMP [10], the present [^{11}C]-donepezil-PET study demonstrated a relatively higher cortical retention of radiotracer, suggesting the existence of alternative binding sites for donepezil other than AChE. Donepezil is reported to have high binding affinity for σ_1 -receptors, which are widely distributed in the brain including the cerebral cortex, hippocampus, and cerebellum [22–24]. A recent human PET study using a σ_1 -receptor-specific radioligand demonstrated prominent reduction of σ_1 -receptor density in the cerebral cortex and cerebellum of AD patients [25]. Thus, concomitant binding of donepezil to σ_1 -receptors might have contributed to the distinctive distribution of [^{11}C]-donepezil we observed in the brain.

Previously, the tracer kinetics of [^{11}C]-donepezil with labelling of the methoxy group at position 6 ([6- ^{11}C -methoxy]-donepezil) were examined in mice and rabbits, to test this agent as a candidate for a PET radioligand [26]. However, the regional brain distribution of this radiotracer did not reflect the distribution of AChE in the brain. In contrast, our previous study yielded successful *in vivo* visualization of AChE by donepezil labelled with ^{11}C at the methoxy group at position 5 ([5- ^{11}C -methoxy]-donepezil)

[5]. The differences between these findings might be attributable to the affinity of unlabelled metabolites to AChE. Indeed, the unlabelled metabolite of [6- ^{11}C -methoxy]-donepezil (M1 in Figure 1) has high binding affinity for AChE ($\text{IC}_{50} = 6.4 \text{ nM}$), resulting in competition for binding between ^{11}C -labelled tracer and unlabelled metabolite, while the metabolite of [5- ^{11}C -methoxy]-donepezil (M2 in Figure 1) exhibits lower affinity of binding to AChE ($\text{IC}_{50} = 1.1 \mu\text{M}$) than M1. [5- ^{11}C -methoxy]-donepezil is thus suitable for detection of AChE *in vivo*. In addition, the specific radioactivity of [5- ^{11}C -methoxy]-donepezil in this study ($111\text{--}354 \text{ GBq } \mu\text{mol}^{-1}$) was higher than that of [6- ^{11}C -methoxy]-donepezil in a previous study [26]. High specific activity of [^{11}C]-donepezil might therefore be another contributing factor of successful visualization of AChE.

In this study, the distribution of donepezil in human brain was successfully visualized using [^{11}C]-donepezil and PET. Graphical analysis by Logan plots can be used to obtain quantitative estimates of specific donepezil binding. AD patients exhibited significant reduction of donepezil distribution, even in the early stages of disease. This imaging technique will be useful as a new surrogate marker for evaluation of treatment with donepezil.

This work was in part supported by Grants-in-Aid for scientific research (No. 17390156 for K. Yanai and 18019004 for N. Okamura) from the Japan Society of Promotion of Science (JSPS) and the Ministry of Education, Culture, Sports, Science and Technology in Japan, as well as by a grant from the Japan Society of Technology (JST) on research and education in 'molecular imaging'. The authors thank the volunteers, Dr Syoichi Watanuki for PET operation and Mrs Kazuko Takeda for taking care of the volunteers.

REFERENCES

- Davies P, Maloney AJ. Selective loss of central cholinergic neurons in Alzheimer's disease. *Lancet* 1976; 2: 1403.
- Coyle JT, Price DL, DeLong MR. Alzheimer's disease: a disorder of cortical cholinergic innervation. *Science* 1983; 219: 1184–90.
- Giacobini E. Cholinesterase inhibitors: from the Calabar bean to Alzheimer therapy. In: Cholinesterases and Cholinesterase Inhibitors, ed. Giacobini E. London: 2000.
- Sugimoto H, Ogura H, Arai Y, Iimura Y, Yamanishi Y. Research and development of donepezil hydrochloride, a new type of acetylcholinesterase inhibitor. *Jpn J Pharmacol* 2002; 89: 7–20.
- Funaki Y, Kato M, Iwata R, Sakurai E, Sakurai E, Tashiro M, Ido T, Yanai K. Evaluation of the binding characteristics of [5-(11) C-methoxy]-donepezil in the rat brain for *in vivo* visualization of acetylcholinesterase. *J Pharmacol Sci* 2003; 91: 105–12.

- 6 Logan J. Graphical analysis of PET data applied to reversible and irreversible tracers. *Nucl Med Biol* 2000; 27: 661-70.
- 7 Kilbourn MR, Snyder SE, Sherman PS, Kuhl DE. *In vivo* studies of acetylcholinesterase activity using a labeled substrate, N-[¹¹C]methylpiperidin-4-yl propionate ([¹¹C]PMP). *Synapse* 1996; 22: 123-31.
- 8 Irie T, Fukushi K, Namba H, Iyo M, Tamagami H, Nagatsuka S, Ikota N. Brain acetylcholinesterase activity: validation of a PET tracer in a rat model of Alzheimer's disease. *J Nucl Med* 1996; 37: 649-55.
- 9 Iyo M, Namba H, Fukushi K, Shinotoh H, Nagatsuka S, Suhara T, Sudo Y, Suzuki K, Irie T. Measurement of acetylcholinesterase by positron emission tomography in the brains of healthy controls and patients with Alzheimer's disease. *Lancet* 1997; 349: 1805-9.
- 10 Kuhl DE, Koeppe RA, Minoshima S, Snyder SE, Ficarò EP, Foster NL, Frey KA, Kilbourn MR. *In vivo* mapping of cerebral acetylcholinesterase activity in aging and Alzheimer's disease. *Neurology* 1999; 52: 691-9.
- 11 Blomqvist G, Tavitian B, Pappata S, Crouzel C, Jobert A, Doignon I, Di Giambardino L. Quantitative measurement of cerebral acetylcholinesterase using [¹¹C]physostigmine and positron emission tomography. *J Cereb Blood Flow Metab* 2001; 21: 114-31.
- 12 Tavitian B, Pappata S, Bonnot-Lours S, Prenant C, Jobert A, Crouzel C, Di Giambardino L. Positron emission tomography study of [¹¹C]methyl-tetrahydroaminoacridine (methyl-tacrine) in baboon brain. *Eur J Pharmacol* 1993; 236: 229-38.
- 13 Bencherif B, Endres CJ, Musachio JL, Villalobos A, Hilton J, Scheffel U, Dannals RF, Williams S, Frost JJ. PET imaging of brain acetylcholinesterase using [¹¹C]CP-126 998, a brain selective enzyme inhibitor. *Synapse* 2002; 45: 1-9.
- 14 Finkelstein Y, Wolff M, Biegon A. Brain acetylcholinesterase after acute parathion poisoning: a comparative quantitative histochemical analysis post mortem. *Ann Neurol* 1988; 24: 252-7.
- 15 Shinotoh H, Aotsuka A, Fukushi K, Nagatsuka S, Tanaka N, Ota T, Tanada S, Irie T. Effect of donepezil on brain acetylcholinesterase activity in patients with AD measured by PET. *Neurology* 2001; 56: 408-10.
- 16 Shiraishi T, Kikuchi T, Fukushi K, Shinotoh H, Nagatsuka S, Tanaka N, Ota T, Sato K, Hirano S, Tanada S, Iyo M, Irie T. Estimation of plasma IC₅₀ of donepezil hydrochloride for brain acetylcholinesterase inhibition in monkey using N-[¹¹C]methylpiperidin-4-yl acetate ([¹¹C]MP4A) and PET. *Neuropsychopharmacology* 2005; 30: 2154-61.
- 17 Sramek JJ, Cutler NR. RBC cholinesterase inhibition: a useful surrogate marker for cholinesterase inhibitor activity in Alzheimer disease therapy? *Alzheimer Dis Assoc Disord* 2000; 14: 216-27.
- 18 Mesulam MM, Geula C. Overlap between acetylcholinesterase-rich and choline acetyltransferase-positive (cholinergic) axons in human cerebral cortex. *Brain Res* 1992; 577: 112-20.
- 19 Shinotoh H, Namba H, Fukushi K, Nagatsuka S, Tanaka N, Aotsuka A, Ota T, Tanada S, Irie T. Progressive loss of cortical acetylcholinesterase activity in association with cognitive decline in Alzheimer's disease: a positron emission tomography study. *Ann Neurol* 2000; 48: 194-200.
- 20 Zubenko GS, Moosy J, Martinez AJ, Rao GR, Kopp U, Hanin I. A brain regional analysis of morphologic and cholinergic abnormalities in Alzheimer's disease. *Arch Neurol* 1989; 46: 634-8.
- 21 Prohovnik I, Perl DP, Davis KL, Libow L, Lesser G, Haroutunian V. Dissociation of neuropathology from severity of dementia in late-onset Alzheimer disease. *Neurology* 2006; 66: 49-55.
- 22 Kato K, Hayako H, Ishihara Y, Marui S, Iwane M, Miyamoto M. TAK-147, an acetylcholinesterase inhibitor, increases choline acetyltransferase activity in cultured rat septal cholinergic neurons. *Neurosci Lett* 1999; 260: 5-8.
- 23 Guitart X, Codony X, Monroy X. Sigma receptors: biology and therapeutic potential. *Psychopharmacology* 2004; 174: 301-19.
- 24 Sakata M, Kimura Y, Naganawa M, Oda K, Ishii K, Chihara K, Ishiwata K. Mapping of human cerebral sigma1 receptors using positron emission tomography and [¹¹C]SA4503. *Neuroimage* 2007; 35: 1-8.
- 25 Hashimoto K, Ishiwata K. Sigma receptor ligands: possible application as therapeutic drugs and as radiopharmaceuticals. *Curr Pharm Des* 2006; 12: 3857-76.
- 26 De Vos F, Santens P, Vermeirsch H, Dewolf I, Dumont F, Slegers G, Dierckx RA, De Reuck J. Pharmacological evaluation of [¹¹C]donepezil as a tracer for visualization of acetylcholinesterase by PET. *Nucl Med Biol* 2000; 27: 745-7.

EDITORIAL

Beyond PIB: the next generation of amyloid-imaging ligands

Hitoshi SHINOTOH and Tetsuya SUHARA

Department of Molecular Neuroimaging, Molecular Imaging Center, National Institute of Radiological Sciences, Chiba, Japan

Correspondence: Dr Tetsuya Suhara MD, PhD, Department of Molecular Neuroimaging, Molecular Imaging Center, National Institute of Radiological Science, 4-9-1 Anagawa, Inage-ku, Chiba 263-8555, Japan

Pittsburgh Compound B (PIB) is the commonly used name for *N*-methyl- ^{11}C -2-(4'-methylaminophenyl)-6-hydroxybenzothiazole (6-OH-BTA-1), an amyloid-imaging ligand that is widely used in the US, Europe, Australia, and Japan. Before Klunk and Mathis¹ developed ^{11}C -PIB successfully at Pittsburgh University, a number of research groups had worked to find appropriate compounds as amyloid-imaging ligands *in vivo*. Attempts to find suitable compounds for positron emission tomography (PET) or single photon emission computed tomography (SPECT) studies started in the early 1990s. Radiolabelled monoclonal antibodies targeted to β -amyloid (A β) peptide were exploited as amyloid-imaging agents *in vivo*.² However, the primary limitation of this approach is that large molecular weight biomolecules cannot efficiently cross the blood–brain barrier (BBB) and bind to amyloid plaques contained within the parenchyma of the Alzheimer's disease (AD) brain. Mathis *et al.*¹ at Pittsburgh University initially focused their attention on Congo red, an amyloid-staining agent widely used in histological studies of post-mortem AD brain tissue sections. Congo red is a large molecule, a negatively charged sulfonate under physiological conditions, and is too hydrophilic to penetrate the BBB. Mathis *et al.*¹ then investigated the binding properties of Chrysamine G, a more lipophilic and potent A β ligand. However, efforts over more than 10 years to develop radiolabelled analogs of Congo red and Chrysamine G as amyloid-imaging agents for PET and SPECT were hampered by the relatively poor brain penetration of these compounds.

The first successful *in vivo* attempt to image A β in the brain of AD patients used PET and the malononitrile derivative ^{18}F -2-(1-((2-fluoroethyl)methyl-amino)-2-naphthyl)ethylidene)malononitrile (^{18}F -FDDNP), which was developed by Agdeppa *et al.*³ at the University of California, Los Angeles.⁴ This ligand is a derivative of 2-dialkylamino-6-acylmalononitrile-substituted naphthalenes (DDNP), which is a hydrophobic, viscosity sensitive fluorescent probe. ^{18}F -FDDNP has a high affinity for both A β and neurofibrillar tangles (NFT). Shoghi-Jadid *et al.*⁴ reported the initial results from PET studies in 2002. The PET images showed high accumulation of radioactivity in the frontal, temporal, and parietal cortex in AD patients following injection of ^{18}F -FDDNP. Unfortunately, signal-to-background ratios are low in the brain with this ligand and ^{18}F -FDDNP PET only showed 9% higher cortical uptake in AD brain than in healthy controls.⁵

Mathis *et al.*¹ then turned their attention to thioflavin T, a dye for amyloid and with a small molecular weight. They removed positively charged heterocyclic nitrogen from thioflavin T to allow it to readily cross the BBB and 6-hydroxylated it for rapid clearance from the brain without A β . The resulting compound, ^{11}C -6-OH BTA-1, was named 'PIB' at the University of Uppsala, where the first clinical study was performed with this ligand and PET. In 2004, Klunk *et al.* reported the initial results of a ^{11}C -PIB PET study in 9 healthy volunteers and 16 patients with AD.⁶ ^{11}C -PIB PET showed a 70% increase in the cerebral cortex in AD patients compared with healthy controls. Many researchers in PET centers in the US, Europe,

Australia, and Japan followed their lead to start PET studies with [^{11}C]-PIB. At present, [^{11}C]-PIB PET studies are underway at seven PET centers in Japan and will soon be started at three others.

The [^{11}C]-PIB PET studies showed that almost all AD patients have high PIB binding in the cerebral cortex,⁵ two-thirds of patients with mild cognitive impairment (MCI) have high PIB binding in the cerebral cortex similar to AD,⁶ 80% of patients with Lewy bodies have high PIB binding in the cerebral cortex,⁷ and 10–20% of healthy elderly people have high PIB binding in the cerebral cortex.⁸ Patients with amyloid angiopathy also have high A β accumulation in the cerebral cortex, especially in the occipital cortex.⁹ Longitudinal studies on healthy controls, MCI patients, and AD patients are underway in several institutions, and are expected to reveal the natural course of amyloid deposition in elderly people and AD.

The third successful *in vivo* attempt to image amyloid in the brain of AD patients, performed in Canada, used the stilbene derivative [^{11}C]-4-*N*-methylamino-4'-hydroxystilbene ([^{11}C]-SB-13).¹⁰ In Japan, Kudo *et al.*¹¹ investigated benzoxazole derivatives as amyloid-imaging ligands and developed [^{11}C]-2-(2-[2-dimethylaminothiazol-5-yl]ethenyl)-6-(2-[fluoro]ethoxy)benzoxazole ([^{11}C]-BF-227) as a PET tracer. [^{11}C]-BF-227 may be unique because this ligand specifically binds to cored or mature plaques, whereas [^{11}C]-PIB seems to bind not only to neuritic plaques, but also to some extent to diffuse plaques.¹² However, these amyloid-imaging compounds have a lower signal-to-background ratio in the brain of AD patients than [^{11}C]-PIB. At present, [^{11}C]-PIB seems to be the best ligand for imaging A β in the AD brain by PET.

Does PIB fulfill all the requirements of an amyloid-imaging ligand in routine clinical studies? Carbon-11 is rapidly decayed, with a short half-life of only 20.4 min, which limits the use of PIB to PET centers with an on-site cyclotron and radiochemistry expertise. Fluorine-18 has a half-life of 110 min, meaning that fluorine-18-labelled compounds, such as [^{18}F]-fluoro-D-deoxyglucose ([^{18}F]-FDG) can be delivered to many PET centers from radiopharmaceutical companies. In the US, 95% of PET centers can receive a supply of an [^{18}F]-compound from radiopharmaceutical companies. In Japan as well, many PET centers are covered by the supply of [^{18}F]-FDG from a radio-

pharmaceutical company. Amyloid-imaging ligands labelled with fluorine-18 would greatly facilitate amyloid imaging with PET and it would be a profitable business.

SPECT is more widely available than PET, based on the fact that SPECT scanners are less expensive. Iodine-123 is a single photon emitter with a half-life of 13 h. $^{99\text{m}}\text{Tc}$ is also a single photon emitter, has a half-life of 6 h, and could be produced at institutions by milking. Therefore, amyloid-imaging ligands labelled with [^{123}I] or [$^{99\text{m}}\text{Tc}$] would also greatly facilitate amyloid imaging.

Several companies are interested in the development of amyloid-imaging ligands labelled with [^{18}F], [^{23}I], or [$^{99\text{m}}\text{Tc}$]. In 2003, GE Healthcare licensed a number of compounds from the University of Pittsburgh, including PIB, and started large multisite trials with fluorine-18-labelled PIB in 2007. Avid Radiopharmaceutical Incorporation is a new venture company specializing in the development of imaging agents for AD and Parkinson's disease. They investigated stilbene derivatives and developed a series of ligands that share common structural features with PIB. Bayer Schering Pharma licensed one of the ligands developed by Avid Inc., known as [^{18}F]-BAY94-9172 or *trans*-4-(*N*-methyl-amino)-4'-(2-[2-(^{18}F)-fluoroethoxy]-ethoxy)-ethoxy-stilbene (also as [^{18}F]-AV1/ZK). [^{18}F]-BAY94-9172 has been used at the Center for PET, Austin Health, in Australia.¹³ PET images similar to [^{11}C]-PIB PET images have been obtained in patients with AD and healthy controls with [^{18}F]-BAY94-9172 and PET. The mean neocortical uptake 90–120 min after injection of [^{18}F]-BAY94-9172 was 57% greater in AD patients than in healthy controls.¹³

[^{23}I]-IMPY was developed as an amyloid-imaging ligand for SPECT.¹ Unfortunately, the signal-to-background ratio in the brain of AD patients is low and there is considerable overlap in the target/cerebellum ratio between healthy controls and patients with AD. The development of better SPECT ligands for A β plaque is well underway.

Apart from amyloid imaging with PET or SPECT, Nakada *et al.*¹⁴ recently reported the direct visualization of A β plaques in patients with AD *in vivo* by magnetic resonance microscopy on a 7T clinical system.

In parallel with the development of amyloid-imaging techniques, clinical trials of many anti-amyloid therapeutic drugs are underway.¹⁵ A Phase III

study with monoclonal antibody therapy (bapineuzumab (AAB-001); Elan Corporation, Athlone, Ireland), is ongoing and this agent may be approved for clinical use within a few years in the US and Europe (see <http://clinicaltrials.gov/ct2/results?term=bapineuzumab>). Several clinical trials of gamma secretase inhibitors or modulators are also underway.

The development of amyloid-imaging techniques and anti-amyloid therapy may dramatically change the clinical treatment of AD within a few years. Elderly people, perhaps from 60 years on, may receive a brain checkup, including amyloid imaging, every 5 years. If they are found to have amyloid deposition in the cerebral cortex, they will then be treated with anti-amyloid drugs. The number of AD patients may decrease markedly if anti-amyloid therapy is proven effective. Although we still do not know whether the amyloid cascade hypothesis is true, we are waiting further developments with high expectations. A new diagnostic-therapeutic paradigm to successfully address AD and its harbinger, MCI-amnesic type, is emerging.

REFERENCES

- Mathis CA, Wang Y, Klunk WE. Imaging β -amyloid plaques and neurofibrillary tangles in the aging human brain. *Curr Pharmaceut Design* 2004; **10**: 1469–1492.
- Majocha RE, Reno JM, Friedland RP, VanHaight C, Lyle LR, Marotta CA. Development of a monoclonal antibody specific for beta/A4 amyloid in Alzheimer's disease brain for application to *in vivo* imaging of amyloid angiopathy. *J Nucl Med* 1992; **33**: 2184–2189.
- Agdeppa ED, Kepe V, Liu J *et al*. Binding characteristics of radiofluorinated 6-dialkylamino-2-naphthylethylidene derivatives as positron emission tomography imaging probes for beta-amyloid plaques in Alzheimer's disease. *J Neurosci* 2001; **21**: RC189.
- Shoghi-Jadid K, Small GW, Agdeppa ED *et al*. Localization of neurofibrillary tangles and beta-amyloid plaques in the brains of living patients with Alzheimer disease. *Am J Geriatr Psychiatry* 2002; **10**: 23–35.
- Small GW, Kepe V, Ercoll LM *et al*. PET of brain amyloid and tau in mild cognitive impairment. *N Engl J Med* 2006; **355**: 2652–2663.
- Klunk WE, Engler H, Nordberg A *et al*. Imaging brain amyloid in Alzheimer's disease with Pittsburgh Compound-B. *Ann Neurol* 2004; **55**: 303–305.
- Rowe CC, Ng S, Ackermann U *et al*. Imaging beta-amyloid burden in aging and dementia. *Neurology* 2007; **68**: 1718–1725.
- Mintun MA, Larossa GN, Sheline YI *et al*. [^{11}C]PIB in a nondemented population: Potential antecedent marker of Alzheimer disease. *Neurology* 2006; **67**: 446–452.
- Johnson KA, Gregas M, Becker JA *et al*. Imaging of amyloid burden and distribution in cerebral amyloid angiopathy. *Ann Neurol* 2007; **62**: 229–234.
- Verhoeff NP, Wilson AA, Takeshita S *et al*. *In-vivo* imaging of Alzheimer disease beta-amyloid with [^{11}C]SB-13 PET. *Am J Geriatr Psychiatry* 2004; **12**: 584–595.
- Kudo Y, Okamura N, Furumoto S *et al*. 2-(2-[2-Dimethylaminothiazol-5-yl]ethenyl)-6-(2-[fluoro]ethoxy) benzoxazole: A novel PET agent for *in vivo* detection of dense amyloid plaques in Alzheimer's disease patients. *J Nucl Med* 2007; **48**: 553–561.
- Lockhart A, Lamb JR, Osredkar T *et al*. PIB is a non-specific imaging marker of amyloid-beta (A β) peptide-related cerebral amyloidosis. *Brain* 2007; **130**: 2607–2615.
- Rowe CC, Ackerman U, Browne W *et al*. Imaging of amyloid beta in Alzheimer's disease with ^{18}F -BAY94-9172, a novel PET tracer: Proof of mechanism. *Lancet Neurol* 2008; **7**: 129–35.
- Nakada T, Matsuzawa H, Igarashi H, Fujii Y, Kwee IL. *In vivo* visualization of senile-plaque-like pathology in Alzheimer's disease patients by MR microscopy on a 7T system. *J Neuroimaging* 2008; **18**: 125–129.
- Salloway S, Mintzer J, Weiner MF, Cummings JL. Disease-modifying therapies in Alzheimer's disease. *Alzheimer Dement* 2008; **4**: 65–79.

1. Alzheimer 病の分子イメージング

放射線医学総合研究所分子イメージングセンター客員協力研究員 篠遠 仁
旭神経内科リハビリテーション病院副院長

key words Alzheimer's disease, amyloid, emission tomography, mild cognitive impairment, dementia with Lewy bodies

要 旨

アミロイドイメージングでは種々のリガンドが開発されている。この中で [^{11}C] PIB をリガンドとして用いた PET 測定は欧米と日本の 20 以上の施設で行われており、Alzheimer 病をはじめとする認知症における所見が確立しつつある。Alzheimer 病の大脳皮質では健常者の 1.5~2.5 倍程度の高い集積がみられる (PIB 陽性)。軽度認知障害では PIB 陽性の症例と、健常者と同様 (PIB 陰性) の症例とがあり 2 群にわかれる。健常高齢者でも約 10% の症例で PIB 陽性例がある。Lewy 小体型認知症においても 6 割程度の症例は PIB 陽性である。前頭側頭型認知症では全例で PIB 陰性であったという報告と一部の症例で PIB 陽性であったという報告とがある。

動 向

Alzheimer 病 (AD) の診断法としてアミロイドイメージングが急速に発展している。 [^{11}C] PIB をリガンドとして用いた PET による測定法は欧米と本邦の 20 以上の施設で臨床応用されており、臨床的有用性が確立しつつある。 [^{11}C] PIB 以外にも種々のリガンドの開発も進み、特に ^{18}F 標識のリガンドが開発され、臨床応用がさらに拡

がる可能性がでてきた。一方、MRI では 7T の装置で AD 患者において造影剤を用いずに直接的に老人斑を描出できたと報告された。

活性化ミクログリアの描出の PET イメージングではこれまで [^{11}C] PK11195 が用いられてきたが、 [^{11}C] PK11195 より特異性の高い [^{11}C] DAA1106 が開発され、今後の応用が期待される。

A. アミロイドイメージング

AD 脳では老人斑と神経原線維変化が 2 つの主要な陽性病変である。老人斑は凝集したアミロイド β ペプチド ($\text{A}\beta_{1-40}$ と $\text{A}\beta_{1-42}$) からなり、 $\text{A}\beta$ ペプチドは互いに結合して β シート構造を形成している。 $\text{A}\beta$ ペプチドは典型的な老人斑の他にびまん性老人斑としても脳実質に沈着する。びまん性老人斑は β シート構造をとっている $\text{A}\beta$ の量が少なく、ゴンゴレッドやチオフラビンによって淡く染色される。脳のアミロイドアンギオパチーは $\text{A}\beta_{1-40}$ のペプチドを多く含んでいる。神経原線維変化の構成要素である過磷酸化されたタウ蛋白や、Lewy 小体、海綿状脳症におけるプリオンもアミロイドの一種である。

現在用いられているアミロイドイメージング剤